EFFECT OF CRACKS ON BENDING STIFFNESS IN CONTINUOUS PAVEMENTS

Adnan Abou-Ayyash, W. Ronald Hudson, and Harvey J. Treybig,
Center for Highway Research, University of Texas at Austin

Transverse contraction joints in rigid pavements were long considered essential to preventing pavement damage from volume-change stresses. Continuously reinforced concrete pavement handles these stresses in another way. It allows the pavement to develop a regular pattern of very fine random cracks. In previous analysis of such pavements, it has been extremely difficult to evaluate the effect of cracks on the load-carrying capacity and subsequent performance of the slab. This paper presents an analytical look at the problem of transverse cracking in continuously reinforced concrete pavements. The influence of these cracks on the longitudinal bending rigidity was studied by using basic moment-curvature relations. A relation was developed that expresses the average moment of inertia due to the effect of the crack as a function of material properties and slab geometric characteristics. Results showed that a significant drop of 80 to 90 percent in the bending rigidity is encountered at crack locations. Furthermore, the development length bond idea was used to specify the slab portion affected by the discontinuity. A procedure to simulate this effect by using the discrete-element method of slab analysis is outlined. The procedure is general and simple to use.

A GENERAL discrete-element method for solution of discontinuous plates and slabs has been developed by Hudson, Matlock, and Stelzer (1, 2). The method is based on a physical model representation of a plate or slab by bars, springs, and torsion bars that are grouped in a system of orthogonal beams. Computer programs developed for the aforementioned method are designated by the acronym SLAB. These programs have the ability to handle complex problems with combinations of load and a variety of discontinuities (cracks and joints) and support conditions.

In previous analyses of rigid pavements, it has been difficult to evaluate the effect of cracks on the bending stiffness and the load-carrying capacity of the slab. This paper describes the use of discrete-element SLAB methods to study the behavior of continuously reinforced concrete pavement (CRCP) including modeling of cracks and joints. The effect of cracks on slab bending stiffness was investigated in this study by using basic moment-curvature relations, which consequently made discrete-element modeling of the crack feasible.

THE PROBLEM AND THE APPROACH

CRCP may be defined as a concrete pavement in which the longitudinal reinforcing steel acts continuously for its length and no transverse joints other than occasional construction joints are installed. In actual practice, the continuity is sometimes interrupted by expansion joints at structures. Except for these, there is technically no limit to the length a CRCP can be.

Transverse contraction joints were long considered essential to preventing pavement damage from volume-change stresses. CRCP takes care of these stresses in another way. It allows the pavement to develop a regular pattern of very fine random transverse

Sponsored by Committee on Rigid Pavement Design.

cracks (Fig. 1). The design concept for this pavement type is to provide sufficient reinforcement to keep the cracks tightly closed and to provide adequate pavement thickness to carry the wheel loads across these tightly closed cracks (3).

Because of volume-change stresses, crack formation in the continuously reinforced pavement slab is inevitable until the expansive materials are perfected. Therefore, a thorough understanding of the behavior of a pavement structure with such discontinuities is needed. The real pavement system, including the cracks, must be analyzed. This can be approximated with reasonable confidence by using the SLAB programs.

Figure 2a shows a cracked portion of CRCP, and Figure 2b shows a variation in the moment of inertia in the cracked region. The exact shape of this curve is not clearly known because of the complexity of the problem. The discrete-element method was applied to the discrete CRCP by using basic moment-curvature relations. In these relations, an average moment of inertia, which simulates the effect of cracks on slab bending stiffness, was determined. Furthermore, the development length bond concept (4) was used to specify the slab portion over which the average inertia could realistically be applied.

ANALYSIS AND MODELING

Theoretical Background

Analytical solutions for two-dimensional plate problems have been discussed by others (5), who characterize three kinds of plate bending: thin plates with small deflections, thin plates with large deflections, and thick plates.

For thin plates with small deflections (i.e., in which the deflection is small in comparison with thickness), a satisfactory approximate theory of bending of a plate by lateral loads can be developed by making the following assumptions:

1. There is no deformation in the plate's middle plane;
2. Points of the plate, which initially lie "normal" to the middle surface of the plate, remain "normal" to the middle surface of the plate after bending; and
3. Normal stresses in the direction transverse to the plate can be disregarded.

With these assumptions, the deflected surface of an isotropic plate is described by the biharmonic equation

$$D[(\partial^4 w/\partial x^4) + 2(\partial^4 w/\partial x^2 \partial y^2) + (\partial^4 w/\partial y^4)] = q \qquad (1)$$

where

D = the bending stiffness of the plate,
w = the deflection (with positive upward), and
q = the lateral load.

A complete discussion of this equation is given elsewhere (5).

For a given set of boundary conditions, solution of this differential equation gives all the information necessary for calculating stresses at any point in the plate. Closed-form solutions of this equation are available for a number of special cases, including homogeneous isotropic plates, which are generally round with finite radii or with infinite dimensions in the x and y directions. The loading conditions in most closed-form solutions are either uniform over the entire plate or concentrated in the center of the plate. As the problem becomes complex, with various combinations of load, support, and stiffness conditions, closed-form solutions are generally not available, and a numerical method must be used to solve the problem. The discrete-element method is such a method.

Figure 3 shows the discrete-element model of the slab, as suggested by Stelzer and Hudson (2). The slab or the rigid pavement structure is replaced by an analogous mechanical model representing all stiffness and support properties of the actual slab. The joints of the model are connected by rigid bars that are in turn interconnected by torsion bars representing the plate twisting stiffness C. The flexible joint models the concentrated bending stiffness D and the effects of Poisson's ratio μ. The modulus of

subgrade support k is represented by independent elastic springs, i.e., the Winkler foundation (6). A problem involving almost any physical combination of loads and restraints applied to a slab, including lateral loads, in-place forces, and applied couples or moments, can be solved. Furthermore, slab discontinuities as well as partial subgrade support can be simulated on the model.

The deflection at each joint is the unknown. The basic equilibrium equations are derived from the free body of a slab joint with all appropriate internal and external forces and reactions. These equations sum the vertical forces at each joint and sum the moments about each individual bar. A complete derivation of these equations and the fourth-difference equations can be found elsewhere (2).

Crack Effect and Method of Attack

Because a discontinuity, such as a joint or crack, creates a change in the moment of inertia or stiffness (Fig. 2), it can be simulated on the discrete model with one of the following methods.

The first method requires a clear determination of stiffness variation in the crack region, which is then divided into increments sufficient to define the effect of the discontinuity. A disadvantage of this method is that it may not be possible to define the stiffness variation in the cracked region accurately enough to yield reasonable results. Furthermore, as the number of increments in either the x or y direction increases, computer time increases, making the solution impractical in some cases.

The second method, which was used in this study, deals with an average value of stiffness that considers the discontinuity effect. The derivation of this average value was solely based on basic moment-curvature relations and is independent of increment length. Hence, the whole structure can be divided into about 15 increments in each direction, and reasonable results can be obtained.

Derivation of Average Moment of Inertia $\overline{I}$

For the determination of average moment of inertia $\overline{I}$, the following assumptions are made:

1. A plane section remains plane before and after bending;
2. A straight-line neutral axis can be assumed to represent the average of the actual variable position of the neutral axis; and
3. At the fine crack location, very slight curvature is needed to bring the two parts of the slab in touch and hence allow the transfer of bending.

With these assumptions in mind, consider a 1-ft wide slab section, as shown in Figure 4 (after Winter et al., 4). Because of the cracks, the actual rigidity of the structure is variable along its length; it is largest between cracks where the tension in the concrete contributes to the rigidity and is smallest at the cracks. For the slab shown in Figure 4, we derive from the basic moment-curvature relation

$$1/\overline{\rho} = M_w/E\overline{I} \tag{2}$$

where

$\overline{\rho}$ = average radius of curvature,
M_w = working moment,
E = modulus of elasticity of concrete, and
$\overline{I}$ = average moment of inertia.

Furthermore, we derive from the strain diagram (Fig. 5)

$$1/\overline{\rho} = \overline{e}_s/[d(1 - K)] = \overline{f}_s/[E_s d(1 - K)] \tag{3}$$

where

$\bar{e}_s$ = average strain in reinforcement,
$\bar{f}_s$ = average stress in reinforcement,
E_s = modulus of elasticity of steel,
d = distance from top compression fiber to the centroid of steel, and

$$K = 2[\sqrt{Pn(1 + Pn)} - Pn] \tag{4}$$

in which

P = percentage of longitudinal reinforcement = (area of steel A_s/gross area of concrete b x t) x 100, and
n = E_s/E.

In Eq. 4, K is a fraction that, when multiplied by d, gives the distance to the neutral axis of the section (Fig. 5). This is based on the cracked transformed section (4). It is worthwhile to note that the area of concrete in the percentage of reinforcement term is the gross area of the section and not, as defined in the equations for reinforced concrete, the width of the section times the distance from extreme compression fiber to the centroid of the steel. In Eq. 4, P should be expressed as a ratio rather than as a percentage.

By combining Eqs. 2 and 3 and solving for $\bar{I}$, we get

$$\bar{I} = M_w nd(1 - K)/\bar{f}_s \tag{5}$$

To determine the average stress in the reinforcement, we must consider the contributing effect of the concrete in tension. Let the average tensile stress of concrete between cracks be expressed as

$$\bar{f}_t = k_1 f_r \tag{6}$$

where

f_r = flexural stress of concrete, and
k_1 = a reduction factor based on experimental results (7).

The part of the resisting moment corresponding to the average tensile stress of concrete $\bar{f}_t$, as shown in Figure 6 (after Yu and Winter, 8), is

$$M' = T_c\,(2t/3) \tag{7}$$

where

T_c = the tensile force in the concrete.

By substituting the value of T_c (Fig. 6) in Eq. 7, we get

$$M' = k_1 f_r bt(t - Kd)/3 \tag{8}$$

Further development of this equation is presented elsewhere (7), where the modulus of rupture (flexural stress at instant of cracking f_r) is expressed in terms of the compressive strength of concrete f_c' (8). In final form

$$M' = 0.1(f_c')^{2/3} bt(t - Kd) \tag{9}$$

Hence, the stress in the reinforcement f_s' corresponding to M' can be computed by

$$f_s' = M'/A_s jd \tag{10}$$

Figure 1. Continuously reinforced concrete pavement.

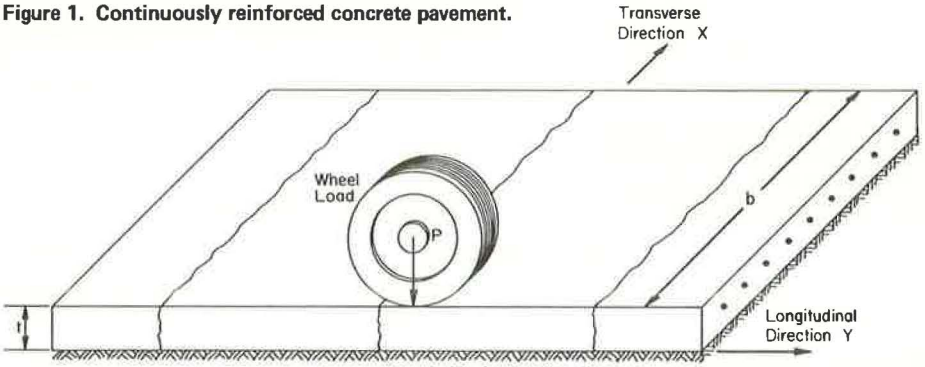

Figure 2. Effect of a discontinuity on the bending rigidity of the slab.

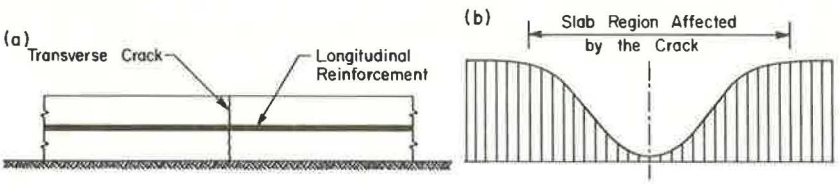

Figure 3. Discrete-element model of a plate or slab.

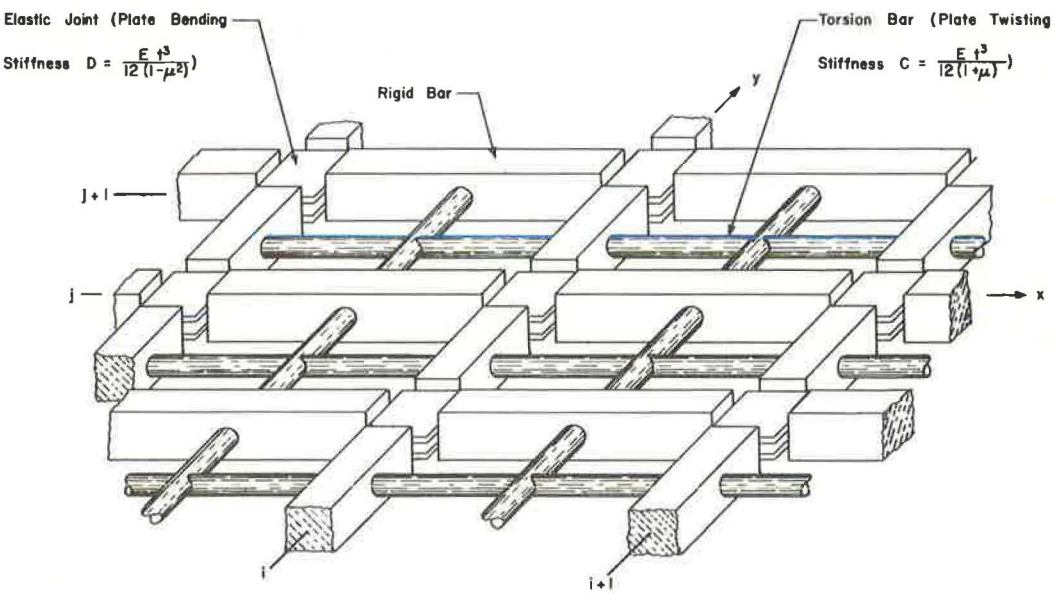

Figure 4. Cracked slab.

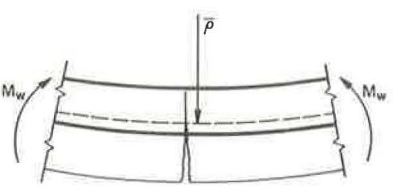

Figure 5. Strain distribution near crack location.

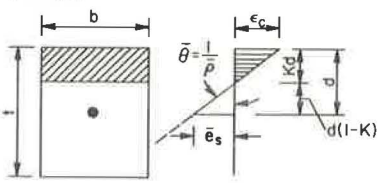

Figure 6. Stress distribution awa from crack location.

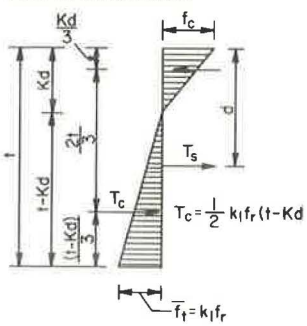

where

f_s' = tensile stress in the steel due to flexural stress in concrete at points away from crack, and
$j = 1 - (K/3)$

But at the cracked section, the steel stress f_s is

$$f_s = M_w/A_s jd \tag{11}$$

The value of the working moment M_w depends on whether the steel or the concrete stress governs (Fig. 7). If the former controls, we derive from Eq. 11

$$M_w = A_s f_s jd$$

where

f_s = the allowable stress in the steel.

On the other hand, if the concrete stress governs, then

$$M_w = f_c Kjbd^2/2 \tag{12}$$

where

f_c = the working compressive stress in the concrete.

By substituting the controlling value of M_w in Eq. 11, we derive the value of the steel stress at the crack and the actual average steel stress $\overline{f}_s$ at the instant of crack initiation:

$$\overline{f}_s = f_s - f_s'$$

Hence, the average moment of inertia is given by

$$\overline{I} = M_w nd(1 - K)/(f_s - f_s') \tag{13}$$

In this equation, the average moment of inertia $\overline{I}$ is expressed in terms of slab geometrical characteristics and material properties. By using the preceding analysis, we get the variation of the percentage of reduction in bending stiffness versus the percentage of reinforcement for different concrete compressive strength values (Fig. 8). Bending stiffness reduction ranged from 80 to 90 percent for the change encountered in the percentage of reinforcement. However, it is important to note the minor influence of the concrete compressive strength on stiffness reduction.

In the development of these curves, the allowable concrete compressive stress was $0.45\ f_c'$, and the allowable tensile steel stress was 0.75 of yield, which is equivalent to a safety factor of 1.33.

Several values of the yield stress, ranging from 40 to 70 psi, were tried. Fortunately, for the range and safety factor in the steel mentioned previously, the variation of the percentage of reduction in bending stiffness was independent of the yield stress. This is due to the fact that the working moment M_w, the lower of the values from Eqs. 11 and 12, was governed by the latter equation where the concrete stress controls. If a lower allowable steel stress is desired (i.e., $< 0.75 f_y$), Eq. 12 may need to be modified.

Region Affected by the Crack

Discontinuities in structural members not only cause severe localized bending stiffness reduction but also influence a certain amount of the area around them. Therefore, after determination of the average moment of inertia and the corresponding reduction in bending stiffness, one more step is required before the discrete-element model of the problem is performed. The length over which the original bending stiffness should be reduced to simulate the effect of the discontinuity must be determined.

A slab portion under the effect of transverse loading (Fig. 9a) is considered. Because the concrete does not resist any tension stresses at the crack, the compression force in the upper concrete fibers has to be balanced by a tensile steel force to maintain equilibrium at that section. In actuality, concrete fails to resist tensile stresses only at a crack. Between cracks, the concrete does resist moderate amounts of tensile stress; this reduces the tensile force in the steel (Fig. 9b), which creates a variable force in the bar. Because the bar must be in equilibrium, this change in bar force is resisted at the contact surface between steel and concrete by equal and opposite forces produced by the bond between steel and concrete. Figure 9c shows a distribution of the bond stress in the cracked region; it should be remembered that the bond development is the rate of change of tension. For the free body of a bar segment shown in Figure 9d, if U is the magnitude of the average bond force per unit length of bar, then $\Sigma F_x = 0$ yields

$$Udx + T - (T + dT) = 0$$

$$\therefore Udx = dT \tag{14}$$

By integrating over the required length, we get

$$U \int_0^a dx = \int_{T_1}^{T_2} dT$$

where

T_1 = tension in steel at some point between cracks, and
T_2 = tension in steel at crack.

Hence,

$$Ua = T_2 - T_1 = A_s f_s - 0$$

$$\therefore a = A_s f_s / U \tag{15}$$

Assuming that the bond force per unit length U is the resultant of shear-type bond stresses u uniformly distributed over the contact area, then

$$U = u\Sigma o \tag{16}$$

where

Σo = the perimeter of the bar(s).

By substituting the value of U in Eq. 15, we derive

$$a = A_s f_s / u\Sigma o \tag{17}$$

Hence, total affected length is as follows:

$$L = 2a \text{ and } L = 2(A_s f_s / u\Sigma o) \tag{18}$$

For the determination of the allowable bond stress u as well as f_s, the ACI 1963 code (Section 1301) specifies the following:

1. For tension bars, the allowable bond stress u is governed by

$$u = 3.4\sqrt{f'c}/\phi \leq 350 \text{ psi} \tag{19}$$

where

ϕ = the bar diameter; and

2. The allowable stress in the steel shall not exceed 24,000 psi.

Discrete-Element Modeling of the Crack Effect

By the previous analysis, the amount of reduction in bending stiffness, as well as the length over which it should be applied, has been determined. In this section, a method for modeling the effect is discussed.

In this method, there are two cases to be considered. In the first case, the region affected by the discontinuity extends over an even number of increments (Fig. 10a). If we assume, for example, that this region is two increments long (L = 2h), it is defined by three stations: two edge stations (i-1, j and i+1, j) and a middle station where the crack is located (i, j). Because the stiffness in the discrete-element model (Fig. 3) is lumped at the elastic joints or station locations in order to simulate the effect previously described, it is necessary to apply the total amount of the previously determined bending stiffness reduction at each middle station (in this case only one, i, j) and half of that amount at each of the boundary or edge stations, namely i-1, j and i+1, j. As an example, if the amount of reduction in bending stiffness is 90 percent of the original full value, 90 percent of the stiffness should be reduced at station i, j and 45 percent at each of the edge stations i-1, j and i+1, j.

In the second case, the area influenced by the crack extends over an odd number of increments, for example, three (L = 3h), as shown in Figure 10b. The main difference between the two cases is the relative position of the ends of the reduced stiffness region and station locations. When there is an even number of increments, a station is located at each of the boundaries or edges of the concerned region, which requires the half-value refinement discussed previously. When there is an odd number of increments, the edges of the reduced stiffness region lie midway between stations, and for modeling the total reduction in bending stiffness is applied at each station (i-1, j, i, j, and i+1, j), with no exception.

For the case where the number of increments is even, it was mentioned that a half value of the stiffness reduction should be applied at the edge stations. To test the sensitivity of the half reduction, we studied several examples. These covered a wide range of thicknesses, moduli of elasticity, crack spacings, and moduli of subgrade reaction. Without exception, neglect of the half-value reduction at the edge stations produced only negligible changes in deflections and principal stresses.

To validate this observation, we considered a problem involving a 20- by 40-ft pavement loaded with a 12-kip concentrated load placed 4 ft from the edge (Fig. 11). The thickness of the pavement was 8 in., and the modulus of subgrade reaction was 100 lb/in.^{3}. The reduction in bending stiffness was applied over a length of 12 in. at each transverse crack location. Figure 11 shows the change in deflection with the increase of the percentage of reduction in bending stiffness; as shown, the rate of change in deflection was almost negligible up to about 50 percent of the stiffness reduction, and then a significant increase was observed. Thus, the application of a half value of stiffness reduction at the edge stations produced almost negligible changes in stresses and deflections.

Therefore, it is recommended that the half bending stiffness reduction at the edge stations be neglected when there is an even number of increments, when the subgrade is not very weak, i.e., $k \approx > 40$ lb/in.^{3}, and when there is no loss in subgrade support.

Suggested Method and Sample Problem

The following step-by-step method is suggested for the application of SLAB programs in the analysis of discontinuities in CRCP:

1. Determine the physical characteristics of the concerned pavement, such as modulus of elasticity, thickness, and percentage of reinforcement;
2. Determine the percentage of reduction in bending stiffness to be applied at crack locations (from Eq. 13 or Fig. 8);

Figure 7. Stress distribution at crack location.

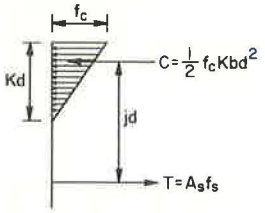

Figure 8. Percentage of reduction in bending stiffness at crack location and percentage of longitudinal reinforcement.

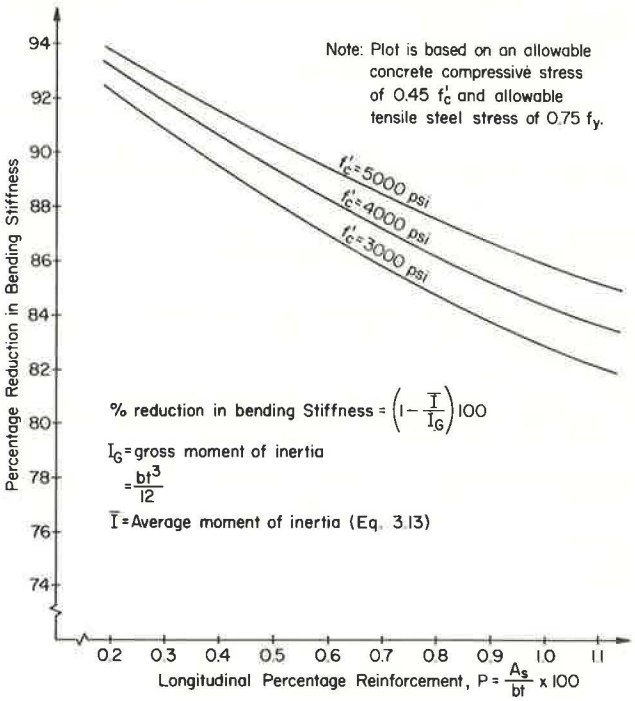

Figure 9. Region affected by the discontinuity.

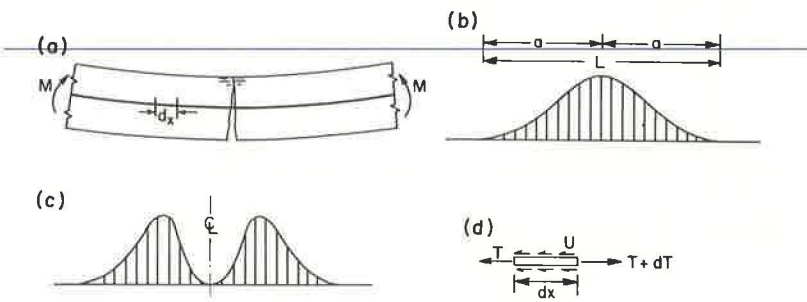

Figure 10. Discrete-element modeling of crack effect.

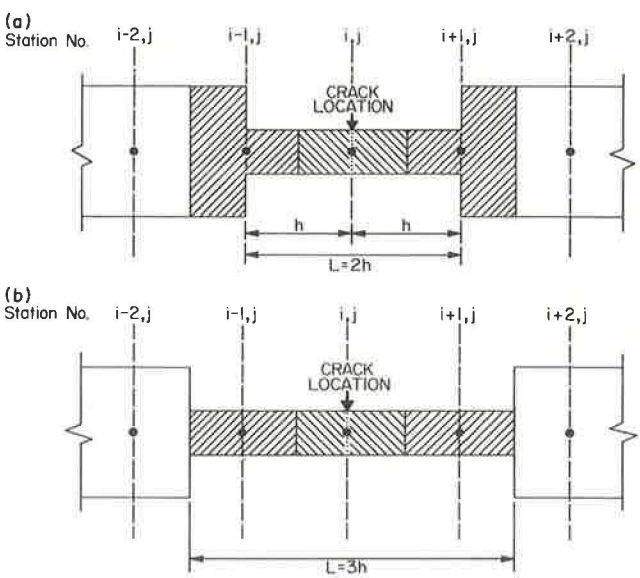

Figure 11. Effect of crack severity on deflection under a 12-kip wheel load.

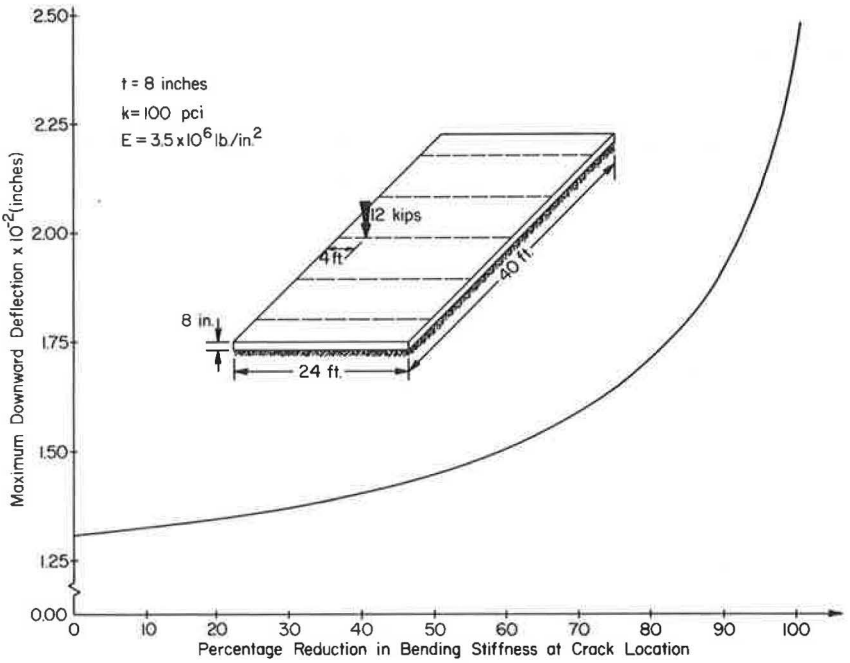

Figure 12. Influence of bending stiffness reduction at cracks on the deflection basin.

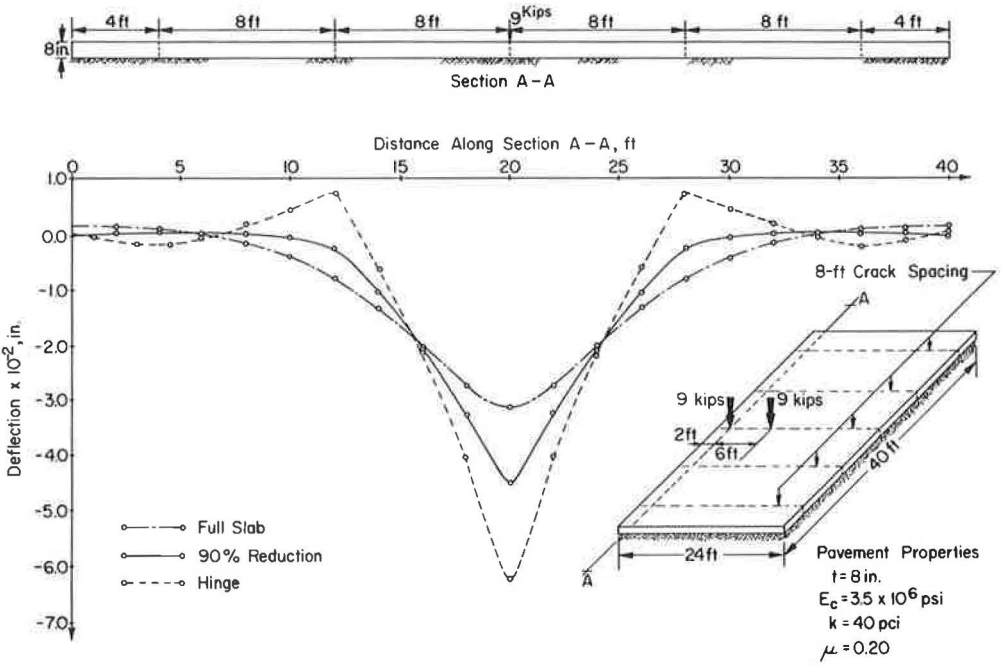

3. Determine the length affected by the discontinuity (from Eq. 18);
4. Decide on the increment length that best matches the slab geometry, as well as the length determined from step 3; and
5. Apply the percentage of stiffness reduction determined in step 2 at each crack location over the length from step 3.

This method is applied on the example problem shown in Figure 12. A 24- by 40-ft slab, loaded with 2, 9,000-lb wheel loads located at 2 and 8 ft from the edge was considered (Fig. 12), and the reduction in bending stiffness was 90 percent over a length of 12 in.

Besides the condition with 90 percent stiffness reduction at the crack location, two other conditions were studied: the hinged condition, where there is zero stiffness at the discontinuity, and the uncracked condition, where the full slab is treated as one piece. The variation in deflections for each of these cases is shown in Figure 12. The effect of the hairline cracks is clearly shown by the 30 percent deflection increase in the 90 percent reduction case over the uncracked case. Furthermore, a comparison of the hinge and the uncracked cases showed a 60 percent increase in maximum deflection for the hinged condition.

Implementation of Results

The development of the application of discrete-element analysis to the continuously reinforced pavement problem will enable designers to more confidently analyze design problems. The SLAB method should be used in a sensitivity analysis of the rigid pavement problem in general. Very specific design analyses can now be made of both jointed pavements and CRCP, which up to this time were approximated by still other techniques. This development will be implemented in the design process.

CONCLUSION

The problem of transverse cracking in CRCP and its influence on the bending rigidity of the slab in the longitudinal direction have been studied by using basic moment-curvature relations. A procedure to simulate this effect by using the discrete-element method is outlined.

The results of the study have indicated that the effect of cracks on the bending rigidity of the slab is highly significant. The reduction in bending stiffness varied from 80 to 90 percent of the original full value for the range of percentage of longitudinal reinforcement studied. Obviously, as the crack width increases, the bending reduction also increases, and ultimately a hinge exists as in the case in a jointed concrete pavement.

ACKNOWLEDGMENTS

This investigation was conducted at the Center for Highway Research, University of Texas at Austin. The authors wish to thank the sponsors, the Texas Highway Department and the Federal Highway Administration. The opinions, findings, and conclusions expressed in this publication are those of the authors and not necessarily those of the Federal Highway Administration.

REFERENCES

1. Hudson, W. R., and Matlock, H. Discontinuous Orthotropic Plates and Slabs. Center for Highway Research, Univ. of Texas at Austin, Res. Rept. 56-6, May 1966.
2. Stelzer, C. F., Jr., and Hudson, W. R. A Direct Computer Solution for Plates and Pavement Slabs. Center for Highway Research, Univ. of Texas at Austin, Res. Rept. 56-9, Oct. 1967.
3. McCullough, B. F. Design Manual for Continuously Reinforced Concrete Pavement. Aug. 1968.
4. Winter, G., Urquhart, L. C., O'Rouke, C. E., and Nilson, A. H. Design of Concrete Structures, 7th Ed. McGraw-Hill, New York, 1964.
5. Timoshenko, S., and Woinowsky-Krieger. Theory of Plates and Shells, 2nd Ed. McGraw-Hill, New York, 1967.

6. Winkler, E. Die Lehre von Elastegatat und Festigkeit. Prague, 1867.
7. Abou-Ayyash, A., and Hudson, W. R. Analysis of Bending Stiffness Variation at Cracks in Continuous Pavements. Center for Highway Research, Univ. of Texas at Austin, Res. Rept. 56-22, Aug. 1971.
8. Yu, Wei-Wen, and Winter, G. Instantaneous and Long-Time Deflections of Reinforced Concrete Beams Under Working Loads. Jour. American Concrete Institute, July 1960.